

Argon Adsorption at 77 K as a Useful Tool for the Elucidation of Pore Connectivity in Ordered Materials with Large Cagelike Mesopores

Michał Kruk and Mietek Jaroniec*

Department of Chemistry, Kent State University, Kent, Ohio 44242

Received December 4, 2002. Revised Manuscript Received April 15, 2003

It is shown that argon adsorption at 77 K is convenient for the elucidation of pore connectivity in ordered materials with large cagelike mesopores and is capable of providing valuable structural information that may not be available from commonly used nitrogen adsorption at 77 K. The discussed approach is based on the phenomenon of pore blocking upon desorption. The nature of this phenomenon is that the capillary evaporation from a particular pore is retarded until either the pore develops an access to the surrounding gas through a continuous path of unfilled pores, or the lower pressure limit of hysteresis for the pore is reached. When the former of these behaviors is observed, the capillary evaporation pressure provides information about the widest continuous path of pore entrances connecting the given pore with the surrounding gas, that is, about the smallest pore entrance size along this widest path. In the case where the capillary evaporation is delayed to the lower limit of hysteresis, it is possible to determine only the upper boundary of the possible pore entrance size. It is shown that argon adsorption at 77 K, for which hysteresis in cylindrical pores is observed for a wider range of pore sizes than for nitrogen at 77 K, is often superior from the point of view of the pore connectivity elucidation, allowing one to probe pore entrance sizes down to ~4.0 nm (compared to ~5.0 nm in the case of nitrogen at 77 K), as estimated using ordered silicas with cylindrical mesopores. The merits of the use of argon at 77 K were demonstrated for the FDU-1 silicas. Conditions favorable for the formation of small pore entrance sizes in FDU-1 were further elucidated, and the lowering of the pore entrance size uniformity with the increase in the initial synthesis temperature was revealed, and bimodal distributions of pore entrances in the samples hydrothermally treated at or above 373 K for extended periods of time were uncovered. Argon adsorption at 77 K is potentially useful for the characterization of pore connectivity in many other large-pore materials.

Introduction

Gas adsorption is a prominent method for determining the specific surface area, pore volume, and pore size distribution (PSD) for mesoporous solids (mesopores are pores of width between 2 and 50 nm).^{1,2} The gas adsorption evaluation of the specific surface area is usually based on the realization that gas atoms or molecules tend to form more or less distinct layers on the surface of the mesoporous solid, which is referred to as a monolayer–multilayer adsorption. The monolayer–multilayer adsorption data are used to determine the monolayer capacity, which is recalculated to obtain the specific surface area, or are compared with adsorption data for a reference solid of known specific surface area, which also allows one to determine the specific surface area for the solid of interest.^{1,2} Determination of the pore volume and PSD from gas adsorption data is usually based on the capillary condensation or evaporation phenomenon.¹ Capillary condensation is the filling of

the core of a mesopore (that is, its inner space that is not occupied by the monolayer or multilayer of gas on its walls) with condensed gas when the pressure reaches a certain value which is related to the mesopore size. Capillary evaporation is the emptying of the pore core as the pressure is decreased. The amount of gas adsorbed after the pores have been completely filled through capillary condensation can be recalculated to obtain the total pore volume, whereas the relation between the capillary condensation or evaporation pressure and the pore size can be used to calculate PSD from the adsorption or desorption branch of the gas isotherm.^{1,2}

In addition to these opportunities in the gas adsorption characterization of porous solids, it is also possible in favorable cases to extract information about the pore connectivity. This additional opportunity stems from the fact that when adsorption–desorption hysteresis is observed on a gas adsorption isotherm, the shape and position of the desorption branch is dependent on the pore connectivity.^{2–14} More specifically, the capillary

* To whom correspondence should be addressed. Tel: (330) 672 3790. Fax: (330) 672 3816. E-mail: jaroniec@kent.edu.

(1) Sing, K. S. W.; Everett, D. H.; Haul, R. A. W.; Moscou, L.; Pierotti, R. A.; Rouquerol, J.; Siemieniewska, T. *Pure Appl. Chem.* **1985**, *57*, 603.

(2) Kruk, M.; Jaroniec, M. *Chem. Mater.* **2001**, *13*, 3169.

(3) Everett, D. H. In *The Solid–Gas Interface*; Flood, E. A., Ed.; Marcel Dekker: New York, 1967; Vol. 2, p 1055.

(4) Broekhoff, J. C. P.; de Boer, J. H. *J. Catal.* **1968**, *10*, 153.

(5) Mason, G. J. *Colloid Interface Sci.* **1992**, *88*, 36.

evaporation pressure from a given pore is dependent not only on its size, but also on its accessibility to the surrounding gas phase. This accessibility is dependent on whether the pores that connect the given pore with the surrounding gas have their cores filled or empty at a particular pressure, which in turn depends on the size and shape of the connecting pores. Therefore, information about the pore connectivity in mesoporous solids can potentially be extracted from the analysis of adsorption–desorption hysteresis loops. Methods suitable for this purpose have already been developed,^{5–8} some of which are based on the percolation theory.^{5–9} However, these methods tend to neglect^{7,8} the single-pore contribution to the adsorption–desorption hysteresis^{6,12,13} and do not make provisions for the lower pressure limit of adsorption–desorption hysteresis, which is experimentally observed.^{1,2}

About 10 years ago, ordered mesoporous materials (OMMs) were reported for the first time.^{15–17} This fascinating new class of porous materials has attracted tremendous interest during the past decade.^{2,18–20} Gas adsorption has become a prominent method for determination of the specific surface area, pore volume, and PSD for OMMs.^{2,18} The structural characterization of OMMs is particularly challenging because these materials often have a high degree of structural perfection and in some cases their structures can be tailored at Angstrom levels of precision and accuracy, whereas many available characterization tools are far from reaching a similar level of precision and accuracy.^{2,10,12} Therefore, OMMs can be used as model solids suitable for the development or refinement of characterization methods, as demonstrated in the case of the PSD calculation for cylindrical pores from gas adsorption data.^{10,21,22} One of the challenges in the characterization of OMMs is the elucidation of their pore connectivity. There are numerous OMMs, including silicas,^{14,23–42} aluminosilicates,⁴³ organosilicas,^{44,45} and non-siliceous

- (6) Ball, P. C.; Evans, R. *Langmuir* **1989**, *5*, 714.
- (7) Liu, H.; Zhang, L.; Seaton, N. A. *J. Colloid Interface Sci.* **1993**, *156*, 285.
- (8) Liu, H.; Seaton, N. A. *Chem. Eng. Sci.* **1994**, *49*, 1869.
- (9) Rojas, F.; Kornhauser, I.; Felipe, C.; Esparza, J. M.; Cordero, S.; Dominguez, A.; Riccardo, J. L. *Phys. Chem. Chem. Phys.* **2002**, *4*, 2346.
- (10) Kruk, M.; Jaroniec, M.; Sayari, A. *Langmuir* **1997**, *13*, 6267.
- (11) Kruk, M.; Jaroniec, M.; Sayari, A. *Adsorption* **2000**, *6*, 47.
- (12) Ravikovich, P. I.; Neimark, A. V. *Langmuir* **2002**, *18*, 1550.
- (13) Ravikovich, P. I.; Neimark, A. V. *Langmuir* **2002**, *18*, 9830.
- (14) Matos, J. R.; Mercuri, L. P.; Kruk, M.; Jaroniec, M. *Langmuir* **2002**, *18*, 884.
- (15) Beck, J. S.; Vartuli, J. C.; Roth, W. J.; Leonowicz, M. E.; Kresge, C. T.; Schmitt, K. D.; Chu, C. T.-W.; Olson, D. H.; Sheppard, E. W.; McCullen, S. B.; Higgins, J. B.; Schlenker, J. L. *J. Am. Chem. Soc.* **1992**, *114*, 10834.
- (16) Yanagisawa, T.; Shimizu, T.; Kuroda, K.; Kato, C. *Bull. Chem. Soc. Jpn.* **1990**, *63*, 988.
- (17) Inagaki, S.; Fukushima, Y.; Kuroda, K. *J. Chem. Soc., Chem. Commun.* **1993**, 680.
- (18) Corma, A. *Chem. Rev.* **1997**, *97*, 2373.
- (19) Ying, J. Y.; Mehnert, C. P.; Wong, M. S. *Angew. Chem., Int. Ed.* **1999**, *38*, 56.
- (20) Stein, A.; Melde, B. J.; Schroden, R. C. *Adv. Mater.* **2000**, *12*, 1403.
- (21) Kruk, M.; Jaroniec, M. *Chem. Mater.* **2000**, *12*, 222.
- (22) Kruk, M.; Jaroniec, M. *J. Phys. Chem. B* **2002**, *106*, 4732.
- (23) Huo, Q.; Margolese, D. I.; Ciesla, U.; Feng, P.; Gier, T. E.; Sieger, P.; Leon, R.; Petroff, P. M.; Schuth, F.; Stucky, G. D. *Nature* **1994**, *368*, 317.
- (24) Huo, Q.; Leon, R.; Petroff, P. M.; Stucky, G. D. *Science* **1995**, *268*, 1324.
- (25) Zhao, D.; Huo, Q.; Feng, J.; Chmelka, B. F.; Stucky, G. D. *J. Am. Chem. Soc.* **1998**, *120*, 6024.

oxides,^{46–48} which exhibit 3-dimensionally (3-D) ordered structures of interconnected cage-like mesopores. Until recently, there were only a few reported successful attempts to elucidate the size of these connecting pores. Two of them^{33,42} involved electron crystallography, which is a powerful method capable of providing the solution for the entire structure of 3-D OMM, including its pore entrance size.⁴² Use of this method led to the evaluation of pore entrance sizes for SBA-1, SBA-6, and SBA-16 silicas.⁴² Another attempt involved the study of changes in the pore accessibility after surface modification with appropriate ligands of different sizes, and led to determination of the pore entrance size for FDU-1 silicas.⁴⁹ A subsequent study of low-pressure adsorption on FDU-1 cast additional light on the opportunities in pore-entrance-size tailoring in the FDU-1 structure.³⁹ Finally, adsorption of molecules of different sizes was employed to elucidate the pore entrance size in SBA-1 and SBA-2 silica samples.⁴⁰

In addition to OMMs with cage-like pores, the pore connectivity elucidation is important for understanding the structures of numerous other OMMs and related materials,^{50–68} for instance those with channel-like

- (26) Zhao, D.; Yang, P.; Melosh, N.; Feng, J.; Chmelka, B. F.; Stucky, G. D. *Adv. Mater.* **1998**, *10*, 1380.
- (27) Yang, P.; Zhao, D.; Chmelka, B. F.; Stucky, G. D. *Chem. Mater.* **1998**, *10*, 2033.
- (28) Zhang, W.; Glomski, B.; Pauly, T. R.; Pinnavaia, T. J. *Chem. Commun.* **1999**, 1803.
- (29) Yu, C.; Yu, Y.; Zhao, D. *Chem. Commun.* **2000**, 575.
- (30) Kim, J. M.; Stucky, G. D. *Chem. Commun.* **2000**, 1159.
- (31) Tattershall, C. E.; Jerome, N. P.; Budd, P. M. *J. Mater. Chem.* **2001**, *11*, 2979.
- (32) Kim, J. M.; Sakamoto, Y.; Hwang, Y. K.; Kwon, Y.-U.; Terasaki, O.; Park, S.-E.; Stucky, G. D. *J. Phys. Chem. B* **2002**, *106*, 2552.
- (33) Sakamoto, Y.; Diaz, I.; Terasaki, O.; Zhao, D.; Perez-Pariente, J.; Kim, J. M.; Stucky, G. D. *J. Phys. Chem. B* **2002**, *106*, 3118.
- (34) El-Safty, S. A.; Evans, J. J. *J. Mater. Chem.* **2002**, *12*, 117.
- (35) Tattershall, C. E.; Aslam, S. J.; Budd, P. M. *J. Mater. Chem.* **2002**, *12*, 2286.
- (36) Van Der Voort, P.; Benjelloun, M.; Vansant, E. F. *J. Phys. Chem. B* **2002**, *106*, 9027.
- (37) Yu, C.; Tian, B.; Fan, J.; Stucky, G. D.; Zhao, D. *J. Am. Chem. Soc.* **2002**, *124*, 4556.
- (38) Tian, B.; Liu, X.; Zhang, Z.; Tu, B.; Zhao, D. *J. Solid State Chem.* **2002**, *167*, 324.
- (39) Matos, J. R.; Kruk, M.; Mercuri, L. P.; Jaroniec, M.; Zhao, L.; Kamiyama, T.; Terasaki, O.; Pinnavaia, T. J.; Liu, Y. *J. Am. Chem. Soc.* **2003**, *125*, 821.
- (40) Garcia-Bennett, A. E.; Williamson, S.; Wright, P. A.; Shannon, I. J. *J. Mater. Chem.* **2002**, *12*, 3533.
- (41) Goltner, C. G.; Berton, B.; Kramer, E.; Antonietti, M. *Chem. Commun.* **1998**, 2287.
- (42) Sakamoto, Y.; Kaneda, M.; Terasaki, O.; Zhao, D. Y.; Kim, J. M.; Stucky, G. D.; Shin, H. J.; Ryoo, R. *Nature* **2000**, *408*, 449.
- (43) Roziere, J.; Brandhorst, M.; Dutartre, R.; Jacquin, M.; Jones, D. J.; Vitse, P.; Zajac, J. *J. Mater. Chem.* **2001**, *11*, 3264.
- (44) Matos, J. R.; Kruk, M.; Mercuri, L. P.; Jaroniec, M.; Asefa, T.; Coombs, N.; Ozin, G. A.; Kamiyama, T.; Terasaki, O. *Chem. Mater.* **2002**, *14*, 1903.
- (45) Cho, E.-B.; Kwon, K.-W.; Char, K. *Chem. Mater.* **2001**, *13*, 3837.
- (46) Yang, P.; Zhao, D.; Margolese, D. I.; Chmelka, B. F.; Stucky, G. D. *Nature* **1998**, *396*, 152.
- (47) Yang, P.; Zhao, D.; Margolese, D. I.; Chmelka, B. F.; Stucky, G. D. *Chem. Mater.* **1999**, *11*, 2813.
- (48) Tian, B.; Yang, H.; Liu, X.; Xie, S.; Yu, C.; Fan, J.; Tu, B.; Zhao, D. *Chem. Commun.* **2002**, 1824.
- (49) Kruk, M.; Antochshuk, V.; Matos, J. R.; Mercuri, L. P.; Jaroniec, M. *J. Am. Chem. Soc.* **2002**, *124*, 768.
- (50) Kramer, E.; Forster, S.; Goltner, C.; Antonietti, M. *Langmuir* **1998**, *14*, 2027.
- (51) Liu, X.; Tian, B.; Yu, C.; Gao, F.; Xie, S.; Tu, B.; Che, R.; Peng, L.-M.; Zhao, D. *Angew. Chem., Int. Ed.* **2002**, *41*, 3876.
- (52) Chan, Y.-T.; Lin, H.-P.; Mou, C.-Y.; Liu, S.-T. *Chem. Commun.* **2002**, 2878.
- (53) Bagshaw, S. A. *J. Mater. Chem.* **2001**, *11*, 831.
- (54) Lukens, W. W., Jr.; Yang, P.; Stucky, G. D. *Chem. Mater.* **2001**, *13*, 28.

pores whose diameters were modified as a result of surface modification^{66,67} or inclusion of guest species.⁶⁸ In all these cases, the detection of constrictions in the OMM structure and the determination of their size is important from the point of view of assessment of transport properties,⁶⁹ molecular sieving properties,^{40,49} the propensity to the pore blocking,⁴⁹ suitability for fabrication of sensors,⁷⁰ templating properties,⁷¹ suitability for immobilization of molecules, clusters, biomolecules,⁷² and so forth. Therefore, there is a need to identify or develop more convenient or more powerful methods for the pore connectivity elucidation.

During a recent symposium on mesostructured materials, we proposed to use argon adsorption at 77 K as a convenient tool for the characterization of constrictions in porous structures.^{73,74} The suitability of argon at 77 K for this purpose was first predicted on the basis of the known adsorption behavior of argon in uniform cylindrical pores of model MCM-41 silicas, and then confirmed experimentally for FDU-1 silicas with cage-like pores. Herein, the conceptual basis of the pore entrance size assessment from desorption data (including data for argon at 77 K) is discussed and its merits are illustrated for FDU-1 silicas with large cagelike pores. In particular, the use of argon adsorption at 77 K allowed us to gain some new and important insights into the FDU-1 pore entrance structure and into the opportunities for its tailoring, which broadened the knowledge gained in our recent extensive study of FDU-1 using transmission electron microscopy, X-ray diffraction, small-angle X-ray scattering, and nitrogen

adsorption.³⁹ Our conclusions about the merits of argon adsorption at 77 K in the pore entrance size analysis are in accord with a very recent experimental and theoretical study of nitrogen, argon, and krypton adsorption in cagelike pores reported by Ravikovich and Neimark.¹³ In particular, these authors arrived at the same estimates of lower limits of pore entrance sizes that can be determined from nitrogen and argon desorption data at 77 K, although our assessment was based on the use of model materials with cylindrical pores, and theirs was based on the interpretation of density functional theory (DFT) data for cylindrical pores and on experimental data for cagelike pores.

Materials and Methods

Materials. FDU-1 silicas were synthesized from tetraethyl orthosilicate (TEOS) in the presence of poly(butylene oxide)-poly(ethylene oxide) triblock copolymer (EO₃₉BO₄₇EO₃₅; B50-6600, Dow) using the synthesis mixture composition reported by Yu et al.²⁹ FDU-1 was identified in our recent study³⁹ as a cubic close-packed structure (*Fm*3*m* space group) with 3-D hexagonal close-packed intergrowth. Earlier electron crystallography studies of a mesoporous silica-based material with *Fm*3*m* structure revealed that each pore in such a structure is connected with twelve neighboring pores.³³ The synthesis of FDU-1 samples was carried out in one or two steps. The first step involved vigorous mixing, either at or above room temperature (up to 353 K), for 1 day. The second step was carried out without stirring in a Teflon-lined autoclave. The details of the synthesis can be found elsewhere.³⁹ The samples are denoted as in ref 39. In particular, FDU-1 silicas synthesized in the one-step synthesis are denoted Tx, where x is the synthesis temperature (in degrees Kelvin). Samples synthesized in the two-step synthesis are denoted TxHy-t, where y is the temperature of the second step of the synthesis, and t is its time in hours ("h") or days ("d"). In cases where more than one sample synthesized under particular conditions was described in ref 39, the sample number is added at the end of the symbol. For example, T298H373-6h2 denotes the second of two FDU-1 samples synthesized at room temperature and heated for 6 h at 373 K.

Measurements. Nitrogen and argon adsorption measurements were performed at 77 K using a Micromeritics ASAP 2010 volumetric adsorption analyzer. Before the measurements, the samples were outgassed under vacuum in the port of the adsorption analyzer for at least 2 h at 473 K. In the case of argon adsorption at 77 K, the relative pressure was calculated as a ratio of the equilibrium vapor pressure to the saturation vapor pressure for the gas–solid equilibrium (measured periodically during the adsorption run).²²

Results and Discussion

Background. *Adsorption in Mesopores.* Before the results of the experimental adsorption studies of FDU-1 and MCM-41 silicas are presented and discussed, it is important to briefly discuss some relevant aspects of gas adsorption in porous media. As the pressure is increased, adsorption in mesopores proceeds via monolayer–multilayer adsorption on the pore walls, followed by the capillary condensation, that is, filling of the pore core with condensed gas.^{1,2} The subsequent pressure decrease results in desorption via the capillary evaporation, which is the emptying of the pore core, followed by the desorption from the multilayer on the pore walls. Hereafter, the mesopore will be referred to as “unfilled”, if it has not been completely filled via capillary condensation, or has already been emptied via capillary

- (55) Yu, C.; Tian, B.; Fan, J.; Stucky, G. D.; Zhao, D. *Chem. Lett.* **2002**, 62.
- (56) Muth, O.; Schellbach, C.; Fröba, M. *Chem. Commun.* **2001**, 2032.
- (57) Burleigh, M. C.; Markowitz, M. A.; Wong, E. M.; Lin, J.-S.; Gaber, B. P. *Chem. Mater.* **2001**, 13, 4411.
- (58) Zhu, H.; Jones, D. J.; Zajac, J.; Dutartre, R.; Rhomari, M.; Roziere, J. *Chem. Mater.* **2002**, 14, 4886.
- (59) Thieme, M.; Schuth, F. *Microporous Mesoporous Mater.* **1999**, 27, 193.
- (60) Wong, M. S.; Jeng, E. S.; Ying, J. Y. *Nano Lett.* **2001**, 1, 637.
- (61) Kriesel, J. W.; Sander, M. S.; Tilley, T. D. *Chem. Mater.* **2001**, 13, 3554.
- (62) Lee, B.; Yamashita, T.; Lu, D.; Kondo, J. N.; Domen, K. *Chem. Mater.* **2002**, 14, 867.
- (63) Lee, J.; Sohn, K.; Hyeon, T. *Chem. Commun.* **2002**, 2674.
- (64) Zakusky, A. S.; Olayo-Valles, R.; Wolf, J. H.; Hillmyer, M. A. *J. Am. Chem. Soc.* **2002**, 124, 12761.
- (65) Van Der Voort, P.; Ravikovich, P. I.; De Jong, K. P.; Benjelloun, M.; Van Bavel, E.; Janssen, A. H.; Neimark, A. V.; Weckhuysen, B. M.; Vansant, E. F. *J. Phys. Chem. B* **2002**, 106, 5873.
- (66) Kruk, M.; Jaroniec, M.; Joo, S. H.; Ryoo, R. *J. Phys. Chem. B* **2003**, 107, 2205.
- (67) Schuth, F.; Wingen, A.; Sauer, J. *Microporous Mesoporous Mater.* **2001**, 44–45, 465.
- (68) Cho, M. S.; Choi, H. J.; Kim, K. Y.; Ahn, W. S. *Macromol. Rapid Commun.* **2002**, 23, 713.
- (69) Fan, J.; Yu, C.; Wang, L.; Sakamoto, Y.; Terasaki, O.; Tu, B.; Zhao, D. In *Abstracts of 3rd International Mesostructured Materials Symposium*, Korean Zeolite Association: Jeju, Korea, July 8–11, 2002; PA-22, p 72.
- (70) Yamada, T.; Zhou, H. S.; Uchida, H.; Tomita, M.; Ueno, Y.; Honma, I.; Asai, K.; Tatsuma, T. *Microporous Mesoporous Mater.* **2002**, 54, 269.
- (71) Yu, C.; Stucky, G. D.; Zhao, D. In *Abstracts of 3rd International Mesostructured Materials Symposium*, Korean Zeolite Association: Jeju, Korea, July 8–11, 2002; PA-4, p 54.
- (72) Han, Y.-J.; Watson, J. T.; Stucky, G. D.; Butler, A. *J. Mol. Catal. B: Enzymatic* **2002**, 17, 1.
- (73) Jaroniec, M.; Kruk, M. In *Abstracts of 3rd International Mesostructured Materials Symposium*, Korean Zeolite Association: Jeju, Korea, July 8–11, 2002; PB-12, p 130.
- (74) Jaroniec, M. In *Abstracts of 3rd International Mesostructured Materials Symposium*, Korean Zeolite Association: Jeju, Korea July 8–11, 2002; KL-14, p 36.

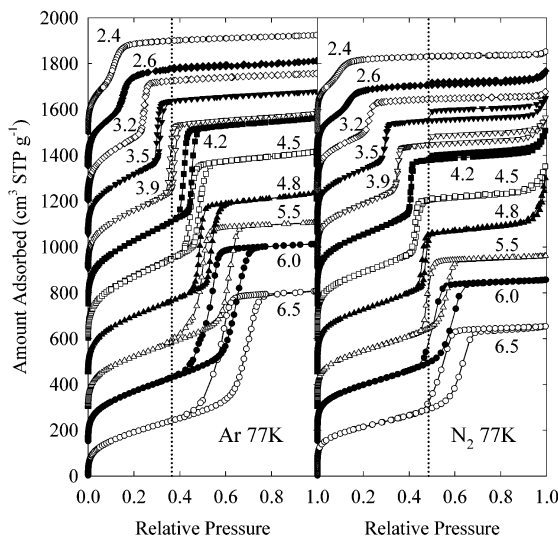


Figure 1. Argon and nitrogen adsorption–desorption isotherms measured at 77 K for a series of eleven MCM-41 silicas with approximately cylindrical pores of diameter 2.4–6.5 nm. The dotted lines indicate the lower limit of adsorption–desorption hysteresis observed in the case of FDU-1 samples for the particular gas. Argon adsorption data are taken from ref 22, whereas nitrogen adsorption data are taken from references listed therein.

evaporation. Otherwise, the pore will be referred to as “filled”. In general, for a given pore geometry, the capillary condensation pressure increase as the pore diameter increases.

Adsorption–Desorption Hysteresis. It has been observed that above a certain pressure limit (hereafter referred to as the lower limit of adsorption–desorption hysteresis), adsorption and desorption branches of gas isotherms for mesoporous adsorbents do not coincide^{1,2} (see Figure 1). This phenomenon is referred to as the adsorption–desorption hysteresis. Numerous experimental and theoretical studies strongly indicate that the adsorption–desorption hysteresis in mesopores has two major causes. One is thermodynamic in nature and is related to the peculiarities of adsorption–desorption behavior in single (isolated) pores.^{6,7,12,13} This behavior manifests itself in a delay of capillary condensation or evaporation or both of these phenomena in a single pore with respect to the equilibrium phase transition for the pore.^{6,12,13} The delay can be understood as the persistence of metastable states on adsorption or desorption or both branches of the hysteresis loop beyond the point of equilibrium between these two branches.

“Pore Blocking” Contribution to the Hysteresis as the Basis of the Pore Entrance Size Assessment. The lack of accessibility of the gas condensed in a given pore to the surrounding gas phase may be another cause of adsorption–desorption hysteresis. This factor is often referred to as the pore blocking effect.^{6,12,14} This lack of accessibility does not appear to have any major influence on the position of the capillary condensation transition,^{12–14} but is well documented to strongly influence the position of the capillary evaporation transition.^{1–14} Namely, at pressures above the lower limit of adsorption–desorption hysteresis, the capillary evaporation from a given pore is delayed when the pore does not have access to the surrounding gas phase through a continuous path

of unfilled pores. Because of that, the extent to which the capillary evaporation is delayed provides an indication whether the cores of pores that connect the given pore with the surrounding gas are filled or not with the condensed gas. This depends on the single-pore behavior of the connecting pores (related to their size and shape) as well as on their accessibility to the surrounding gas. The pressure at which the delayed capillary evaporation from the given pore takes place reflects the pressure of capillary evaporation from the connecting pores (provided these pores have unrestricted access to the surrounding gas phase). Therefore, the latter pressure can be used to elucidate the diameter of the connecting pores, if their characteristic single-pore adsorption–desorption behavior is known. Taking into account the connectivity of the entire pore system, the pressure at which the delayed capillary evaporation takes place from a given pore reflects the size of the narrowest entrance along the widest path that connects the given pore with the surrounding. However, the above considerations are only valid above the lower limit of adsorption–desorption hysteresis, because the capillary evaporation from a given pore is not delayed beyond the lower limit of hysteresis regardless of the state of the connecting pores (except for the cases where the hysteresis is related to kinetics of adsorption–desorption processes or to swelling of an adsorbent, which is not considered here). It can thus be concluded that the capillary evaporation pressure for a given pore depends on the size of its connecting pores rather than on the size of the given pore itself, which opens an opportunity for the assessment of the size of the connecting pores from the analysis of desorption branches of gas isotherms.^{13,14,75} However, in the cases where the capillary evaporation is delayed to the lower limit of hysteresis, one can merely infer that the connecting pores are of diameter smaller than or equal to the pore diameter corresponding to the lower pressure limit of hysteresis.^{13,14,54}

Adsorption–Desorption Behavior of Single Cylindrical Pores as a Model of Adsorption–Desorption in the Connecting Pores. In the case of an ordered mesoporous material with large cage-like pores, one can envision a model in which the ordered cages are connected with one another by pores that are approximately cylindrical in shape. This assumption, which was already tacitly employed in earlier considerations advanced by us¹⁴ and others,^{13,54} allows one to use the vast knowledge of the adsorption–desorption behavior in cylindrical pores to predict the adsorption–desorption behavior of the connecting pores. This is a remarkable opportunity, because the cylindrical shape is the only pore shape that has been a subject of extensive experimental adsorption studies using model mesoporous solids, such as MCM-41.^{10,21,22,76} The assumption about the cylindrical shape of the connecting pores is certainly an approximation, but it appears to be an acceptable one in light of the recently published structural solution for the large-pore SBA-16 silica.⁴² It appears that the connecting pores in this case are approximately cylindrical, although they are short and their diameter is not constant, being the

(75) Lukens, W. W., Jr.; Schmidt-Winkel, P.; Zhao, D.; Feng, J.; Stucky, G. D. *Langmuir* **1999**, *15*, 5403.

(76) Ravikovitch, P. I.; Neimark, A. V. *Colloids Surf. A* **2001**, *187–188*, 11.

smallest in the middle of the connecting pore and increasing to some extent as this pore merges with the mesopore cage.

Shown in Figure 1 are argon and nitrogen adsorption isotherms acquired at 77 K for MCM-41 silicas with pore diameters from 2.4 to 6.5 nm. In cases of both adsorbates, the same pattern of adsorption–desorption behavior is observed. Multilayer adsorption that takes place at lower pressures is followed by the capillary condensation at pressures gradually and systematically increasing with the pore diameter. Adsorption–desorption isotherms for smaller pores are reversible, but adsorption–desorption hysteresis is observed for larger pore diameters. It is notable that in the case of argon, hysteresis disappears for pores of diameters between 3.2 and 3.5 nm, which is appreciably smaller than the lowest diameter for which hysteresis is observed for nitrogen (somewhere between 3.9 and 4.2 nm; the hysteresis loop for 4.2 nm MCM-41 is too narrow to be seen clearly in Figure 1). Because the adsorption–desorption hysteresis for argon at 77 K extends to appreciably smaller pore sizes than for nitrogen at 77 K, the former experimental conditions appear to be suitable to probe an appreciably wider range of pore entrance sizes.^{73,74}

The dotted lines in Figure 1 denote the lower limits of hysteresis for argon and nitrogen at 77 K observed for FDU-1 silicas^{29,39} with large (10–14 nm diam.) cagelike mesopores. In the cases of argon and nitrogen at 77 K, the lower limits of hysteresis for the large-pore cages (relative pressures of about 0.36–0.37 and 0.48–0.49, respectively; see Figures 2 and 3) correspond to the pressure of capillary evaporation from cylindrical pores of diameters about 3.9 nm and about 5.0 nm, respectively. It should be noted that MCM-41 silicas with pores of diameter up to 4.8 nm were much more highly ordered than MCM-41 silicas with pores of size 5.5 nm or larger.²² Therefore, it appears to be more accurate to assess the diameter of an ideal cylindrical pore that would exhibit capillary evaporation at a relative pressure of 0.48–0.49 from the extrapolation of the behavior for the more uniform, smaller-pore MCM-41 samples, than from the behavior of the less ordered 5.5 nm MCM-41. The results discussed above point to the prospects of elucidation of pore entrance sizes down to about 4.0 nm from argon adsorption data at 77 K, compared to sizes down to ~5.0 nm from nitrogen adsorption data at 77 K.^{73,74} Lowering of the “detection” limit by 1 nm by replacing the nitrogen with argon at 77 K is significant for the characterization of OMMs, whose pore entrances may be uniform in size and tailorabile,^{40,42,49} and may fall into the range that can be characterized on the basis of the hysteresis behavior of argon at 77 K, but not nitrogen at 77 K, as will be shown below. Moreover, other known methods for the pore entrance size elucidation may be either invalid for the considered size range or much more elaborate and time-consuming than the adsorption–desorption method considered here. Note that just before this work was submitted for publication, Ravikovich and Neimark reported the same estimates of lower limits of pore entrance sizes which can be elucidated on the basis of nitrogen and argon adsorption–desorption hysteresis loops at 77 K.¹³ These authors based

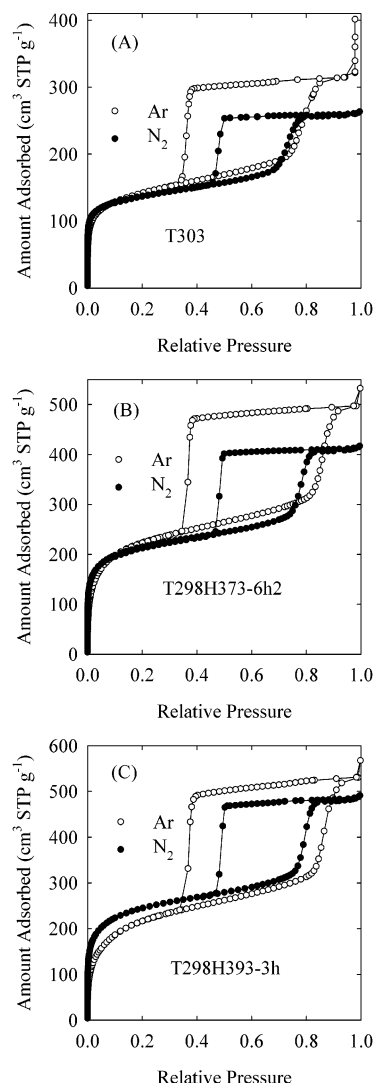


Figure 2. Comparison of argon and nitrogen adsorption–desorption isotherms at 77 K for selected FDU-1 silicas that exhibited the capillary evaporation from the ordered pore cages at the lower limit of adsorption–desorption hysteresis for both argon and nitrogen (nitrogen data for T298H393-3h are taken from ref 39).

their assessment on the results of their DFT calculations for cylindrical pores and their experimental studies of materials with cagelike pores.¹³

Also note that the connecting pores are much shorter than the pores of MCM-41. It is known that for pores of a given diameter, the capillary evaporation transition shifts to higher pressure as the pore length is reduced.^{13,77} Consequently, an assumption that adsorption–desorption behavior of a connecting pore that has a certain diameter of its narrowest part (this diameter will be referred to as the pore entrance size) can be modeled by using a cylindrical pore of this diameter is approximate in nature, as the former pore would exhibit somewhat higher capillary condensation–evaporation pressure. Anyway, this appears to be the best approximation that one can make to relate the behavior of the connecting pores to the known behavior of model pores of simple geometry.

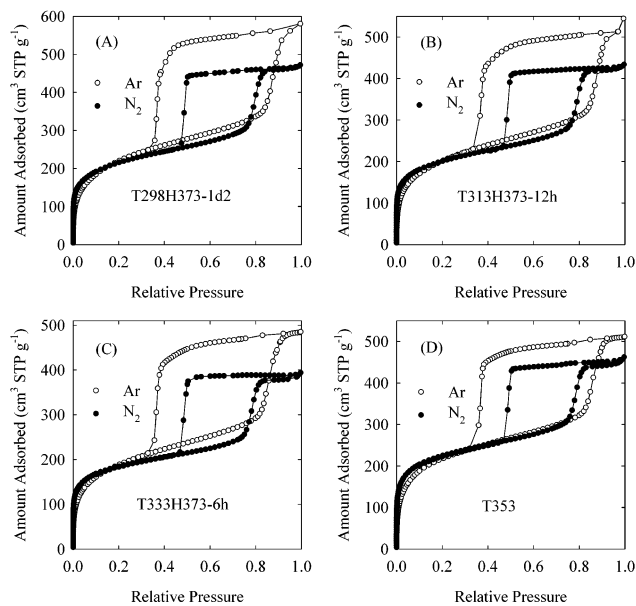


Figure 3. Comparison of argon and nitrogen adsorption–desorption isotherms at 77 K for selected FDU-1 silicas that exhibited the capillary evaporation of nitrogen from the ordered pore cages at the lower limit of adsorption–desorption hysteresis (nitrogen data for T353 are taken from ref 39).

Application to Ordered Materials with Large Cagelike Pores. *Test for Samples of Known Pore Entrance Sizes.* There are only two reports that provide reliable pore entrance size estimates for ordered materials with large cagelike pores^{42,49} (determinations based on the position of the desorption branch of the isotherm, which happened to be located at the lower limit of hysteresis, are obviously considered herein as unreliable). The first one⁴² is the study of an SBA-16 silica sample, for which the pore entrance diameter was assessed to be 2.3 nm using the electron crystallography method. This study also included results for an SBA-6 silica sample, whose structure featured two kinds of mesopore cages with entrances of two different sizes. The other study⁴⁹ concerned FDU-1 silica, for which an average pore entrance diameter was assessed to be about 1.3 nm for a sample synthesized at room temperature (T303), and about 2.4 nm for a sample synthesized at room temperature and subsequently subjected to the hydrothermal treatment at 373 K (T298H373-6h2). These pore entrance size estimates were based on studies of the pore accessibility after surface modifications with ligands of gradually increasing sizes. In the cases of T303 and T298H373-6h2, these studies indicated that there are no pore entrances of diameters above 1.9 and 2.9 nm, respectively. Nitrogen and argon isotherms at 77 K for these two FDU-1 samples are shown in Figure 2 (A) and (B). These isotherms feature wide hysteresis loops (compare with Figure 1) which close at the lower limit of hysteresis. This behavior is consistent with our argument presented above that the pore entrances of diameters above ~4 nm (for argon at 77 K) and ~5 nm (for nitrogen at 77 K) would have to be present to allow for the capillary evaporation from large cagelike mesopores above the lower pressure limit of hysteresis.

Conditions for the Formation of FDU-1 with Pore Entrances Exclusively Below ~4 nm. Argon adsorption

isotherms at 77 K were measured for a wide range of FDU-1 silicas synthesized at different temperatures in one-step and two-step syntheses, as described elsewhere.³⁹ It was found that the capillary evaporation took place at the lower limit of hysteresis, and thus pore entrances were of size exclusively below about 4 nm, for samples synthesized in one step at temperatures up to 333 K. For samples synthesized at room temperature and subsequently hydrothermally treated, the same behavior was generally observed at lower temperatures or for shorter hydrothermal treatment times. In particular, essentially no evidence for the development of pore entrances above 4 nm was inferred from argon data for samples subjected to heating at (i) 333 K for 2 days; (ii) 353 K for 2 days; (iii) 373 K for 12 h; or (iv) 393 K for 3 h (T273H393-3h; see Figure 2 (C)).

Conditions for the Formation of FDU-1 with Pore Entrances Exclusively Below ~5 nm, But with Some Entrances Above ~4 nm. For some FDU-1 silicas, the capillary evaporation of nitrogen at 77 K from primary mesopores was delayed to the lower limit of adsorption–desorption hysteresis, but the onset of the capillary evaporation of argon at 77 K was above the corresponding lower limit of hysteresis (see Figure 3). A similar case has recently been reported and discussed by Ravikovich and Neimark with similar conclusions regarding the pore entrance sizes.¹³ On the basis of the discussion presented above, these samples are expected to exhibit pore entrance sizes exclusively below ~5 nm with a fraction of pore entrances above ~4 nm. This group of samples includes those synthesized at (i) room temperature and hydrothermally treated for 1 day at 373 K (T298H373-1d2); (ii) 313 K and treated for 12 h at 373 K (T313H373-12h); (iii) 333 K and treated for 6 h at 373 K (T333H373-6h); and (iv) 353 K with no hydrothermal treatment (T353). It is interesting to note that the samples synthesized initially at particular temperatures without the subsequent hydrothermal treatment (T313, T333) or hydrothermally treated for shorter periods of time (T313H373-6h) exhibited pore entrances exclusively below ~4 nm, as inferred from argon adsorption isotherms. On the other hand, samples hydrothermally treated for longer times (for 48 h or more after the initial synthesis at room temperature, and for 24 h after the initial synthesis at 313 K) exhibited a fraction of pore entrances above ~5 nm, as seen from nitrogen adsorption.³⁹ It is important to note that the time after which the development of the pore entrances of diameter above ~4 nm was observed decreased as the temperature of the first step of the synthesis increased. Moreover, the decline of the desorption branches of argon isotherms above the lower limit of hysteresis was more gradual for samples initially kept at higher temperature (see Figure 3). This finding strongly suggests that the FDU-1 samples synthesized initially at lower temperature exhibit a narrower pore entrance size distribution, so the self-assembly of FDU-1 above room temperature is not beneficial from the point of view of the pore entrance size uniformity. This conclusion was not apparent from nitrogen adsorption results.

Formation of FDU-1 Silicas with Larger Pore Entrance Sizes. As shown elsewhere using nitrogen ad-

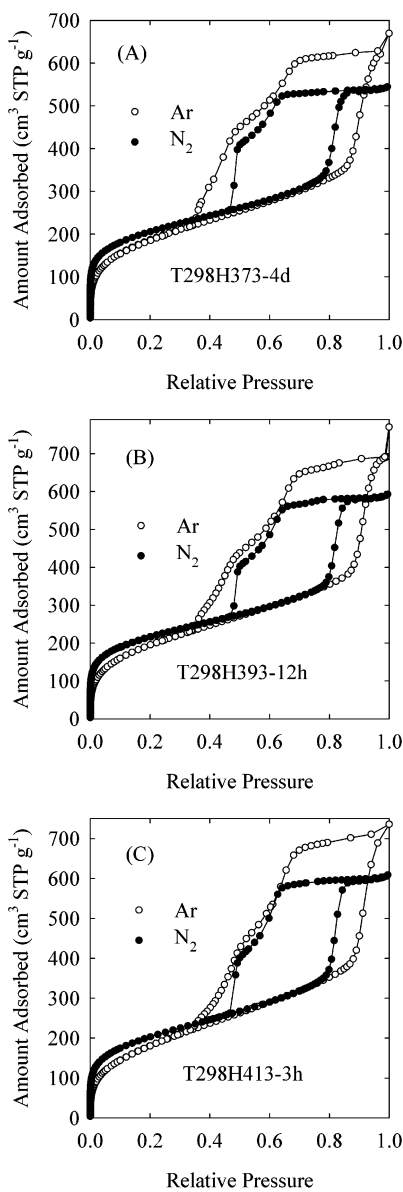


Figure 4. Comparison of argon and nitrogen adsorption–desorption isotherms at 77 K for FDU-1 silicas that were prepared at different hydrothermal treatment times and temperatures, but exhibited a similar adsorption–desorption behavior with two steps on desorption branches of hysteresis loops (nitrogen data are taken from ref 39).

sorption at 77 K,³⁹ the increase in the hydrothermal treatment time at higher temperature (373 K or higher) allows one to enlarge the FDU-1 pore entrance size well beyond ~ 5 nm. However, it was evident that the enlarged pore entrances were not uniform in size. Herein, the evidence is presented that the size distribution of the entrances is actually bimodal and quite narrowly defined when the first step of the synthesis is performed at room temperature. Shown in Figure 4 are nitrogen and argon adsorption isotherms at 77 K for samples hydrothermally treated at (i) 373 K for 4 days (T298H373-4d); (ii) 393 K for 12 h (T298H393-12h); and (iii) 413 K for 3 h (T298H413-3h). Despite the fact that the hydrothermal treatment times were very different for these three samples, their nitrogen adsorption properties appeared to be similar, as noted elsewhere.³⁹ However, the desorption branches of all these nitrogen

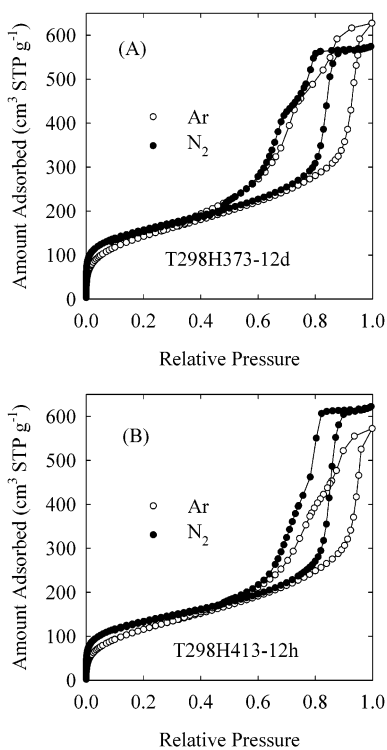


Figure 5. Comparison of argon and nitrogen adsorption–desorption isotherms at 77 K for FDU-1 silicas that were hydrothermally treated for extended periods of time at high temperature (nitrogen data for T298H413-12h are taken from ref 39).

isotherms exhibited significant declines at the lower limit of hysteresis, so it was not possible to make a fully meaningful comparison on the basis of these data, as inferred for instance from the examples discussed earlier. The examination of argon adsorption isotherms showed that the pore connectivity in the three samples indeed appears to be similar. Namely, the argon isotherms for these samples were similar and exhibited capillary evaporation with two steps. Both steps were located primarily above the lower limit of hysteresis, so the argon results allow for a meaningful comparison and thus provide strong evidence for the similarity in the pore connectivity for the three samples considered. It can be inferred that there are two dominant sizes of pore entrances in these samples. However, the estimation of their relative population is not straightforward. If the larger entrances are randomly distributed throughout the ordered structure, their population may actually be small. This is because each large-pore cage of FDU-1 is likely to be connected with its 12 nearest neighbors,³⁹ forming a structure with very high average pore connectivity (the latter is the number of connections per one cagelike pore). This high connectivity implies that even a small population of larger pore entrances may form percolation pathways (continuous passages) from an appreciable fraction of the cagelike pores to the surrounding gas.⁸ It is important to emphasize here that shapes of desorption branches of hysteresis loops observed for nitrogen and argon adsorption above the corresponding lower limits of hysteresis were very similar (see Figure 4). This confirms our contention that the material's structure rather than properties of a particular gas has a major influence on the desorption

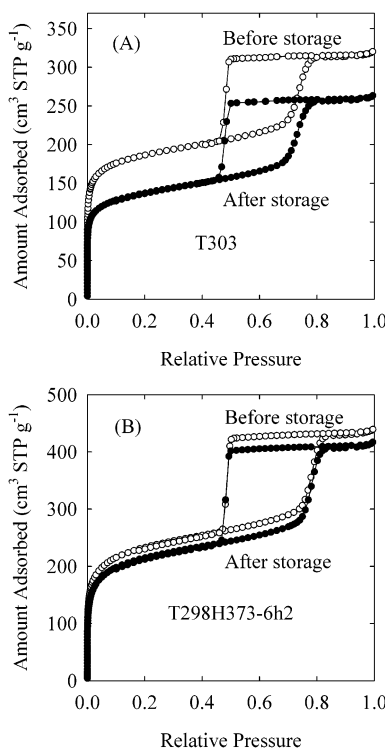


Figure 6. Comparison of nitrogen adsorption isotherms for two FDU-1 samples before and after storage in closed bottles for 8–10 months (data before storage are taken from ref 39).

behavior above the lower limit of hysteresis, although the properties of the particular gas may have some impact on the width of the hysteresis loops (which tend to be wider in the case of argon when compared to nitrogen at 77 K).

Note that in the case presented above, the formation of a similar structure with a two-step desorption behavior was accelerated by about 36 times by an increase in temperature by 40 K (from 373 to 413 K). It is also notable that the two-step desorption behavior persisted as the pore entrances were further enlarged. As can be seen in Figure 5, nitrogen adsorption isotherms for FDU-1 samples hydrothermally treated for relatively long times (12 days at 373 K; 12 h at 413 K) exhibited much narrower hysteresis loops, but still two separate steps could be distinguished on the desorption branches. In these cases, argon adsorption isotherms were not fully informative, because a fraction of the mesoporous cages in these samples was too large to exhibit capillary condensation of argon at 77 K. This manifested itself in the fact that the pore volumes that could be derived from argon data were appreciably smaller (especially for T298H413-12h) than those assessed from nitrogen data. It is known that argon does not exhibit capillary condensation in pores of diameters larger than about 15 nm.^{22,78} This limit was estimated for cylindrical pores²² and may be slightly higher for spherical pores, such as those in FDU-1.

Prospective Applications. The examples discussed above illustrate the merits of using argon adsorption at 77 K in the characterization of silicas with large cagelike pores. This method is also useful in the

characterization of materials with large channel-like pores with constrictions, and many other materials mentioned in the Introduction. For instance, argon at 77 K was successfully used⁶⁶ to gain important insights into the structures of plugged hexagonal templated silicas.⁶⁵

Note on Stability of FDU-1 During Storage. FDU-1 is known to be exceptionally hydrothermally stable.²⁹ However, its adsorption capacity actually decreases upon storage. This decrease was found to be quite large in some cases (up to about 20% after about a year of storage under ambient air in a sealed bottle; see Figure 6 (A)), but was moderate or small in other cases, especially for some samples hydrothermally treated at or above 373 K (see Figure 6 (B)). A minor decrease in the adsorption capacity for FDU-1 after two years of storage was already reported by Ravikovich and Neimark.¹³ This decrease is attributable to the adsorption of water vapor from the air in the framework micropores of FDU-1.³⁹ These micropores can become inaccessible as a result of irreversible water adsorption and subsequent aging of the material upon storage. The loss of adsorption capacity usually affects the uptake at lower pressures, but has little effect on adsorption at higher pressures (see Figure 6). Thus, these results suggest that the excellent hydrothermal stability of FDU-1²⁹ can be understood as the stability of its periodic structure, which does not imply the stability of adsorption properties of framework micropores.

Conclusions

The present study allows us to draw the following important conclusions. Argon adsorption at 77 K provides enhanced opportunities in the elucidation of connectivity of large cagelike pores from desorption branches of hysteresis loops. This is in agreement with the results reported very recently by Ravikovich and Neimark.¹³ Using argon adsorption at 77 K, it was possible to demonstrate that in the case of FDU-1 synthesis, the increase in the initial synthesis temperature is detrimental for the formation of uniformly sized pore entrances. On the other hand, materials with quite similar structures with bimodal pore entrance distributions were found to form for FDU-1 synthesized at room temperature and subjected to the hydrothermal treatment at different temperatures from 373 to 413 K, although the formation of the particular structure required a much shorter time at higher temperature. The analysis of argon adsorption data also allowed us to uncover the common bimodal nature of pore entrance structures in the FDU-1 samples subjected to the hydrothermal treatment at different times. Another important conclusion stems from the fact that the potential of argon at 77 K in the pore entrance size elucidation was identified on the basis of the notion of “pore blocking” on desorption, and the analysis of experimental data for cylindrical pores, which are largely or completely free of pore blocking. This prediction capability provides a strong confirmation of the “pore blocking” mechanism of delayed desorption in porous media.

Acknowledgment. M.J. acknowledges support by NSF Grant CHE-0093707. We thank Dr. Rene Geiger from Dow Chemicals for providing the triblock copolymer.